

## Influence of a magnetic field on the propagation of ultrashort optical pulses in anisotropic optical media with carbon nanotubes

N. N. Konobeeva, M. B. Belonenko

Volgograd State University, University avenue, 100, Volgograd, 400062, Russia

yana\_nn@volsu.ru, belonenko@volsu.ru

**PACS 78.20.Fm, 73.63.Fg**

**DOI 10.17586/2220-8054-2021-12-4-430-435**

In this paper, we investigate the interaction of ultrashort pulses with anisotropic optical media with carbon nanotubes in the presence of a magnetic field. Based on Maxwell's equations, taking into account the second polarization of the light wave, an effective equation for the vector potential of the electromagnetic field is obtained. The dependence of the pulse shape on the magnetic field is revealed, and the Fourier spectra of the pulse are analyzed.

**Keywords:** magnetic field, anisotropic media, carbon nanotubes.

*Received: 2 June 2021*

*Revised: 30 June 2021*

### 1. Introduction

To solve many practical problems, it is necessary to form a powerful electromagnetic pulse with specified characteristics. In this case, an important issue is the study of the pulse's behavior in a medium under the action of the strong external fields [1]. Note that the magnetic field can be used to control the properties of optical pulses, which is confirmed by the Faraday effect and the magneto-optical Kerr effect [2]. In this context, media containing carbon nanotubes with their stabilizing effect have a high potential for application in the development of optoelectronic devices [3]. We have studied the effect of external constant magnetic and alternating electric fields on the ultrashort pulse propagation in CNTs [4, 5], but without taking into account the anisotropy of the medium, which can have a significant effect on the character of pulse propagation. Therefore, the problem of the correct accounting the optically anisotropic properties of a nonlinear medium naturally arises. These properties can lead to various interesting effects, for example, the Zakharov–Benny resonance [6].

Since the works [7, 8], the stable propagation of optical pulses in the CNT array has been shown repeatedly. As an example, we cite recent papers on this topic [9, 10]. In previous studies, we took into account only one (linear) polarization of light, when the nanotube axis was parallel to the electric field vector. Here, we take into account the second polarization, as well as different values of the velocity components. In this work, we study the dynamics of a three-dimensional ultrashort optical pulse in a dielectric anisotropic crystal with CNTs under the action of a constant magnetic field.

### 2. Model and basic equations

We consider an array of carbon nanotubes immersed in an anisotropic dielectric medium (crystal). The OX, OY and OZ axes are aligned with the crystal axes. The CNT axis lies in the XOY plane and makes an angle  $\alpha$  with the OX axis (Fig. 1). We investigate the propagation of three-dimensional ultrashort electromagnetic pulses in the array of zigzag carbon nanotubes. We consider only semiconductor carbon nanotubes to avoid the effects associated with intraband absorption. The magnetic field  $H$  is directed along the CNT axis. Under the action of the electric field  $E$  directed along the OX axis, a current begins to flow in the CNTs and a field appears along the other axis, the OY axis. Note, in this paper, we consider a positive crystal [11]. There are several ways to obtain well-oriented nanotubes in a dielectric matrix. It is important that the distance between CNTs is much greater than the distances between atoms. For example, one of the methods is induced anisotropy using external fields due to the Kerr effect. Moreover, we consider the pulse field to be much larger than the external field responsible for the anisotropy. Another method is media of polar molecules. It should be noted that our approach is a generalization, but it is also suitable for an isotropic medium.

The vector potential has the form:  $\mathbf{A} = (A_x(x, y, z, t), A_y(x, y, z, t), 0)$ , the electric current density is:  $\mathbf{j} = (j_x(x, y, z, t), j_y(x, y, z, t), 0)$ .

We write the three-dimensional wave equation for the electric field component directed at an angle to the CNT axis (taking into account the calibration:  $\mathbf{E} = -\partial A/c\partial t$ ):

$$\frac{1}{c^2} \frac{\partial^2 A}{\partial t^2} = \frac{\partial^2 A}{\partial x^2} + \frac{\partial^2 A}{\partial y^2} + \frac{\partial^2 A}{\partial z^2} + \frac{4\pi}{c} j(A), \quad (1)$$

where  $c$  is the light velocity.

Next, we go over to a cylindrical coordinate system and rewrite equation (1) into two components of the vector potential:

$$\begin{aligned} \frac{1}{v_0^2} \frac{\partial^2 A_x}{\partial t^2} &= \frac{1}{r} \frac{\partial}{\partial r} \left( r \frac{\partial A_x}{\partial r} \right) + \frac{\partial^2 A_x}{\partial z^2} + \frac{1}{r^2} \frac{\partial^2 A_x}{\partial \varphi^2} + \frac{4\pi}{c} j_x(A_x, A_y), \\ \frac{1}{v_e^2} \frac{\partial^2 A_y}{\partial t^2} &= \frac{1}{r} \frac{\partial}{\partial r} \left( r \frac{\partial A_y}{\partial r} \right) + \frac{\partial^2 A_y}{\partial z^2} + \frac{1}{r^2} \frac{\partial^2 A_y}{\partial \varphi^2} + \frac{4\pi}{c} j_y(A_x, A_y), \end{aligned} \quad (2)$$

$$v_0 = c/n_x, \quad v_e = c/n_y,$$

$r, z, \varphi$  are the cylindrical coordinates;  $n_x, n_y$  are the refractive indices for  $x$  polarization and for  $y$  polarization respectively,  $v_0$  is the velocity of an ordinary ray,  $v_e$  is the velocity of an extraordinary ray. Earlier in [12, 13], we have shown that there is a damping of azimuthal harmonics during the propagation of an electromagnetic wave in an array of CNTs. Therefore, we neglect the derivative with respect to the angle.

The standard expression for the current density along the CNTs axis can be written as [14]:

$$j = 2e \sum_{s=1}^m \int v_s(p) \cdot f(p, s) dp, \quad (3)$$

where  $e$  is the electron charge, hereinafter  $\hbar = 1$ , the integration is carried out over the first Brillouin zone,  $p$  is the projection of the quasi-momentum of the conduction electron along the axis of the nanotube,  $v_s(p) = \partial \varepsilon_s(p)/\partial p$  is the electron velocity,  $f(p, s)$  is the Fermi distribution,  $\varepsilon_s(p)$  is the dispersion law, which describes the properties of electrons of CNTs and takes into account a magnetic field [15]:

$$\varepsilon_s(p) = \pm \gamma_0 \sqrt{1 + 4 \cos(ap_z) \cos\left(\frac{\pi}{n} \left(s + \frac{\Phi}{\Phi_0}\right)\right) + 4 \cos^2\left(\frac{\pi}{n} \left(s + \frac{\Phi}{\Phi_0}\right)\right)}, \quad (4)$$

where  $s = 1, 2, \dots, n$ , CNTs type is  $(n, 0)$ ,  $\gamma_0 \approx 2.7$  eV,  $a = 3b/2\hbar$ ,  $b$  is the distance between adjacent carbon atoms,  $\Phi$  is the magnetic flux through the cross section of CNT,  $\Phi_0 = h/e \approx 2.068 \cdot 10^{-15}$  Wb is the magnetic flux quantum [16]. Because the magnetic field is codirectional to the nanotube axis, then  $\Phi = B \cdot S$ , where  $S$  is the CNT cross-sectional area,  $B$  is the modulus of the magnetic induction vector.

Based on calculations in [14], we assume that the derivative with respect to the angle is zero. In this case, we obtain a system of the effective equations for the components of the vector potential, taking into account the transition to the cylindrical coordinate system:

$$\begin{cases} \frac{1}{r} \frac{\partial}{\partial r} \left( r \frac{\partial A_x}{\partial r} \right) + \frac{\partial^2 A_x}{\partial z^2} - \frac{1}{v_0^2} \frac{\partial^2 A_x}{\partial t^2} + \frac{4en_0\gamma_0 a \cdot \cos \alpha}{c} \sum_{q=1}^{\infty} b_q \sin(\tilde{A}) = 0, \\ \frac{1}{r} \frac{\partial}{\partial r} \left( r \frac{\partial A_y}{\partial r} \right) + \frac{\partial^2 A_y}{\partial z^2} - \frac{1}{v_e^2} \frac{\partial^2 A_y}{\partial t^2} + \frac{4en_0\gamma_0 a \cdot \sin \alpha}{c} \sum_{q=1}^{\infty} b_q \sin(\tilde{A}) = 0, \\ \tilde{A} = \frac{aeq(A_x \cos \alpha + A_y \sin \alpha)}{c}, \end{cases} \quad (5)$$

$n_0$  is the electron concentration:

$$b_q = \sum_s a_{sq} \int_{ZB} dp \cdot \cos(pq) \frac{\exp(-\varepsilon_s(p)/k_B T)}{1 + \exp(-\varepsilon_s(p)/k_B T)}, \quad (6)$$

$k_B$  is the Boltzmann constant,  $T$  is the temperature,  $a_{sq}$  is the coefficients in the expansion of the electron dispersion law (4) as a Fourier series:

$$\varepsilon_s(p) = \frac{1}{2\pi} \sum_{s=1}^m \sum_{q=1}^{\infty} a_{sq} \cos(pq), \quad (7)$$

$$a_{sq} = \int_{ZB} dp \cdot \cos(pq) \varepsilon_s(p). \quad (8)$$

Note, due to a decrease in the coefficients  $b_q$  (6), with an increase in  $q$ , we can restrict ourselves to the first 15 nonvanishing terms [17].

The system of equations (5) is solved numerically. We use an explicit finite-difference three-layer scheme of the “cross” type with the following initial conditions:

$$\begin{aligned} A_x &= Q \cdot \exp\left(-\left(\frac{z}{l_z^2}\right)^2\right) \exp\left(-\frac{x^2 + y^2}{l_r^2}\right), \\ \frac{d}{dt}A_x &= \frac{2v_0Q}{l_z^2} \cdot \exp\left(-\left(\frac{z}{l_z^2}\right)^2\right) \exp\left(-\frac{x^2 + y^2}{l_r^2}\right), \\ A_y &= 0, \quad \frac{d}{dt}A_y = 0 \end{aligned} \quad (9)$$

where  $Q$  is the initial amplitude of the electromagnetic pulse,  $l_z, l_r$  determine the pulse width along the  $z$  and  $r$  directions, respectively,  $z_0$  is the initial coordinate of the pulse center along the axis  $z$ .

### 3. Results and discussion

Further, we make numerical calculations at the following system parameters: CNT of type is (80, 0), coefficients  $b_q$ , are calculated at the temperature  $T = 293$  K [18]. It should be noted some points of our model. The substrate field is not taken into account. Distances between adjacent carbon nanotubes are much larger than their diameter. The magnetic field is directed strictly along the axis of the nanotubes. We consider pulses from the near-IR, with a duration of 1 period, and a width of 2 wavelengths. Examples of the pulse producing, see in [19, 20].

The evolution of the electromagnetic field during its propagation over the sample in the presence of a constant magnetic field is shown in Fig. 2. We presented the field intensity  $I$ , which is determined according to the formula:

$$I = \frac{1}{c^2} \left( \frac{\partial A_x}{\partial t} \right)^2. \quad (10)$$

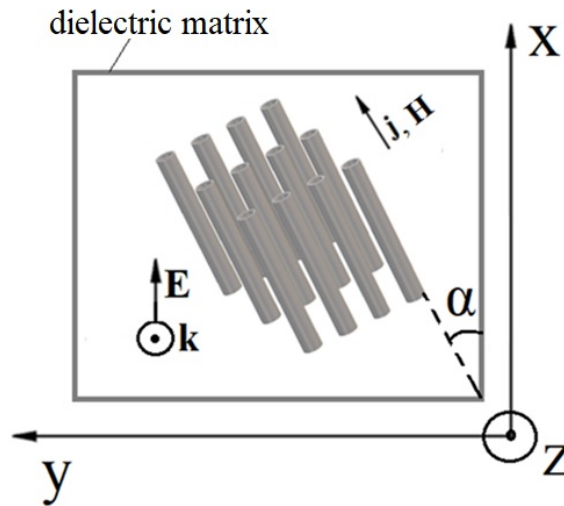


FIG. 1. The geometry of the problem

Figure 2 shows that dispersive spreading of the pulse is observed. Despite this, the pulse is localized in the propagation direction. The dispersion spreading of the pulse is essential here and it is associated with the fact that both field components ( $E_x$  and  $E_y$ ) are taken into account in the problem. This is the most important difference between this problem and the problems considered earlier.

The dependence of the pulse width  $l_z$  (which is defined as the distance at which its intensity drops by half of the intensity at the center) is shown in Fig. 3.

The essential point here is that the pulse component that was initially excited is broadened least of all. It can be associated with the fact that nonlinear effects act there from the very beginning, which compensate for the spreading.

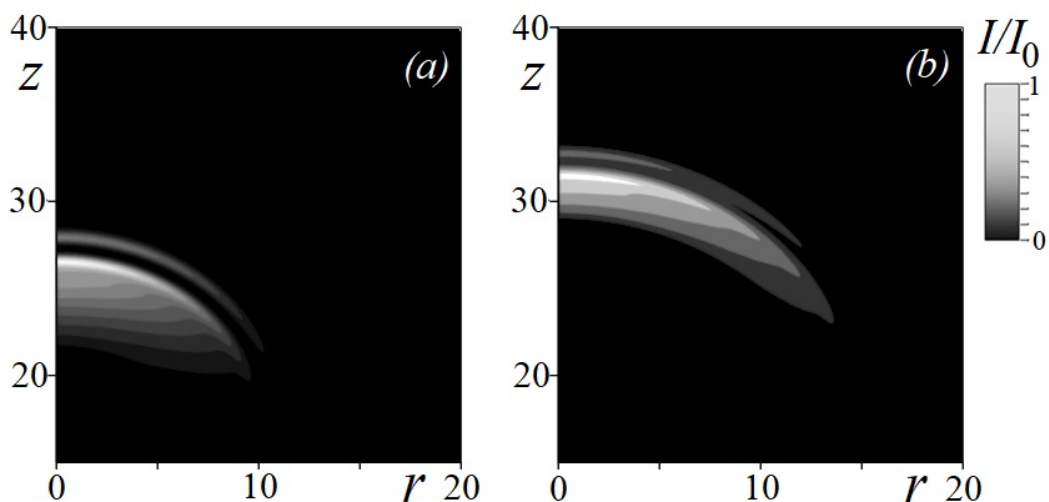


FIG. 2. Evolution of the pulse: a)  $t = 6.5$ ; b)  $t = 9.5$ . The nondimensional unit along the  $r$  and  $z$  axes corresponds to  $2 \cdot 10^{-5}$  m, in time  $10^{-14}$  s.  $I_0$  is the field intensity at  $t = 0$ .

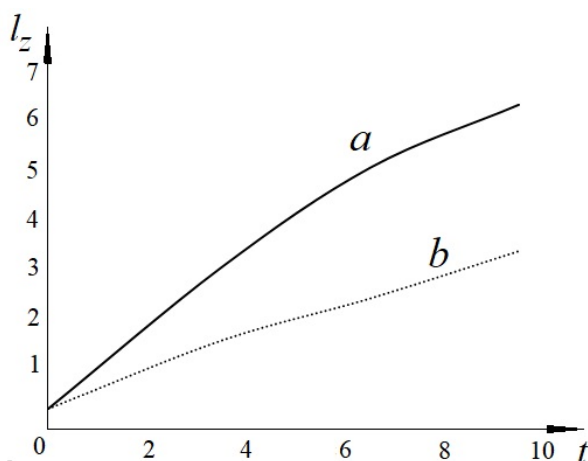


FIG. 3. Dependence of the pulse width on time: a) for the component  $E_y$ ; b) for the component  $E_x$ . The nondimensional unit along the vertical axis corresponds to  $2 \cdot 10^{-5}$  m, in time  $10^{-14}$  s.

At the same time, this dependence explain us why the broadening is much stronger than in previous works, for example [9, 12]. This is due to the presence of the second component of the electric field vector, which makes its own contribution.

The influence of the angle between the electric field  $E_x$  with the carbon nanotubes axis on the dynamics of the pulse propagation is shown in Fig. 4.

It can be seen, that the greater the magnetic field, the higher the field intensity for different angles of inclination of the CNT to the crystal axis.

The influence of the magnetic field on the pulse dynamics is presented in Fig. 5.

It follows from Figs. 4 and 5 that the amplitude and shape of the pulse can be controlled both by the angle at which the CNT array is located in the dielectric matrix, and by the magnitude of the magnetic field. It can be seen, that by choosing in a certain way the angle  $\alpha$  and the magnitude of the magnetic field, we can control the longitudinal dispersion of the pulse.

Let us analyze the shape of the Fourier spectrum ( $\omega$  is the angular frequency) of the pulse at a fixed time (Fig. 6).

Figure 6 shows, that for sharp angles,  $\alpha$ , between the nanotube axis and the crystal axis, additional peaks appear in the Fourier spectrum. It indicates the generation of additional harmonics. Note, when the magnitude of the constant magnetic field increases, the number of these peaks also increases. By varying the magnitude of the external magnetic

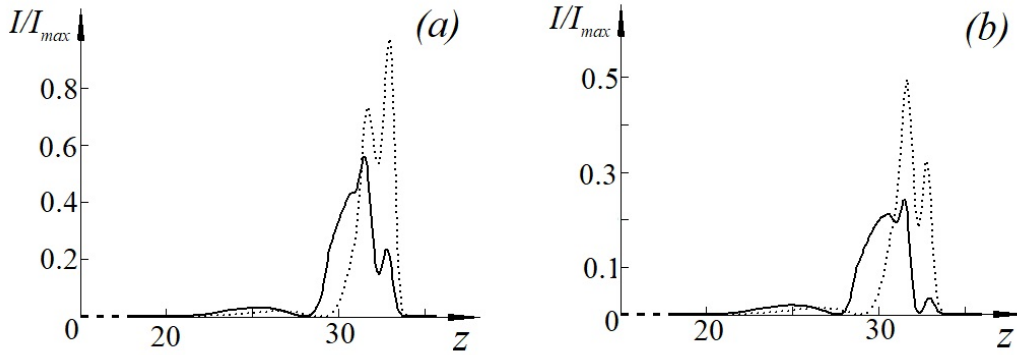


FIG. 4. Dependence of the electric field intensity  $E_x$  on the  $z$  coordinate for the time instant  $t = 9.5$  (slices at  $r = 0$ ): (a)  $\alpha = 0.75$  rad; (b)  $\alpha = 1.05$  rad. For the dashed line, the magnetic field is 2 times greater than for the solid one. The nondimensional unit along the  $z$  axis corresponds to  $2 \cdot 10^{-5}$  m, the dimensionless unit on time is  $10^{-14}$  s.  $I_{max}$  is the maximum value of field intensity at  $t = 9.5$ .

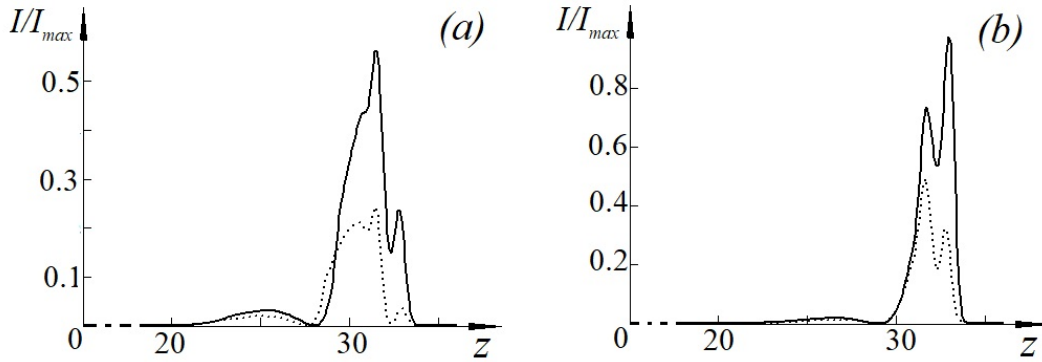


FIG. 5. Dependence of the electric field intensity  $E_x$  on the  $z$  coordinate for the time instant 9.5 (slices at  $r = 0$ ). For the Fig. (b) the magnetic field is 2 times greater than for (a). The solid line corresponds to  $\alpha = 0.75$  rad, the dashed line –  $\alpha = 1.05$  rad. The nondimensional unit along the  $z$ -axis corresponds to  $2 \cdot 10^{-5}$  m, the dimensionless unit on time is  $10^{-14}$  s.  $I_{max}$  is the maximum value of field intensity at  $t = 9.5$  (at the following parameters:  $\alpha = 0.75$  rad,  $\Phi/\Phi_0 = n/2$ ).

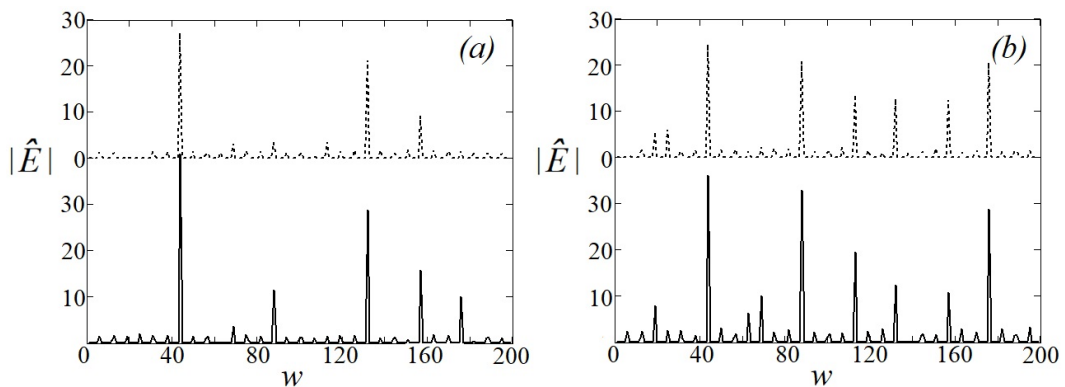


FIG. 6. Absolute values of Fourier spectra at time  $t = 9.5 \cdot 10^{-14}$  s for several values of  $\alpha$  and the magnetic field. For the Fig. (b) the magnetic field is 2 times greater than for (a). The dashed line corresponds to  $\alpha = 1.05$  rad, the solid line corresponds to  $\alpha = 0.75$  rad. The unit on the  $\omega$  axis corresponds to  $10^{13}$  s $^{-1}$ , on the axis  $|E| = 10^7$  V/m.

field (as well as the angle  $\alpha$ ), it is possible to achieve the effective generation of the second harmonic, or vice versa, to suppress this generation and make the generation of the third harmonic more efficient. It is also possible to control the generation of higher harmonics and harmonics at intermediate frequencies. This is undoubtedly important for practical applications, since it allows one to make a device on a single crystal for generating harmonics controlled by a magnetic field. We note another application. The value of the magnetic field applied to the sample can be determined from the harmonic output. That is this effect can be useful for optical magnetism sensors.

#### 4. Conclusion

This study reports three key results, which have some practical applications in the harmonic generation:

- (1) A model of propagation of ultrashort optical pulses in an anisotropic optical media with carbon nanotubes in the presence of a magnetic field is proposed.
- (2) The magnitude of the magnetic field makes it possible to change both the amplitude and the shape of the pulse during its propagation over the sample.
- (3) The magnitude of the magnetic field effectively controls the output of optical harmonics.

#### Acknowledgements

N. N. Konobeeva acknowledges support from the Ministry of Science and Higher Education of the Russian Federation, RF President's Grants Council Grant No. MD-3173.2021.1.2 (agreement 075-15-2021-337 dated 20.04.2021).

#### References

- [1] Mihalache D. Localized structures in optical and matter-wave media: A selection of recent studies. *Rom. Rep. Phys.*, 2021, **73**, 403.
- [2] Kerr J. On rotation of the plane of polarization by reflection from the pole of a magnet. *Philosophical Magazine*, 1877, **3** (19), P. 321–343.
- [3] Sadykov N.R., Muratov E.T., Pilipenko I.A., Aporoski A.V. Wavefunctions and energy eigenvalues of charge carriers in zigzag carbon nanotubes and in armchair nanoribbons in the vicinity of Dirac point under the influence of longitudinal electric field. *Physica E: Low-Dimensional Systems and Nanostructures*, 2020, **120**, 114071.
- [4] Belonenko M.B., Glazov S.Y., Mescheryakova N.E. Effect of an AC electric field on the conductance of single-wall semiconductor-type carbon nanotubes. *Semiconductors*, 2010, **44** (9), P. 1211–1216.
- [5] Konobeeva N.N., Belonenko M.B. Dynamics of ultimately short electromagnetic pulses in chiral carbon nanotubes in the presence of an external field. *Technical Physics*, 2014, **59**, P. 1749–1752.
- [6] Sazonov S.V., Sobolevskii A.F. Continuous Stokes self-scattering of an optical pulse in a uniaxial crystal in the case of Zakharov—Benney resonance. *Quantum Electronics*, 2005, **35**, P. 1019–1026.
- [7] Belonenko M.B., Lebedev N.G., Popov A.S. Two-dimensional light bullets in an array of carbon nanotubes. *JETP Letters*, 2010, **91**, P. 461–465.
- [8] Leblond H., Mihalache D. Spatiotemporal optical solitons in carbon nanotube arrays. *Phys. Rev. A*, 2012, **86** (4), 043832.
- [9] Fedorov E.G., Zhukov A.V., et al. Propagation of three-dimensional bipolar ultrashort electromagnetic pulses in an inhomogeneous array of carbon nanotubes. *Phys. Rev. A*, 2018, **97** (4), 043814.
- [10] Fedorov E.G., Zhukov A.V., et al. External light control of three-dimensional ultrashort far-infrared pulses in an inhomogeneous array of carbon nanotubes. *Phys. Rev. B*, 2021, **103** (8), 085111.
- [11] Matveev A.N. *Optics*. Mir, Moscow, 1988, 446 p.
- [12] Konobeeva N.N., Fedorov E.G., et al. Stabilization of ultrashort pulses by external pumping in an array of carbon nanotubes subject to piezoelectric effects. *J. Appl. Phys.*, 2019, **126**, 203103.
- [13] Konobeeva N.N., Belonenko M.B. Propagation of three-dimensional extremely short optical pulses in germanene in the presence of an external electric field. *Optics and Spectroscopy*, 2017, **123**, P. 425–429.
- [14] Zhukov A.V., Bouffanais R., Fedorov E.G., Belonenko M.B. Three-dimensional electromagnetic breathers in carbon nanotubes with the field inhomogeneity along their axes. *J. Appl. Phys.*, 2013, **114**, 143106.
- [15] Eletsii A.V. Carbon nanotubes. *Physics-Uspeski*, 1997, **40**, P. 899–924.
- [16] Ovchinnikov A.A., Atrazhev V.V. Magnetic susceptibility of multilayered carbon nanotubes. *Physics of the Solid State*, 1998, **40**, P. 1769–1773.
- [17] Belonenko M.B., Demushkina E.V., Lebedev N.G. Electromagnetic solitons in a system of carbon nanotubes. *J. Rus. Las. Res.*, 2006, **27**, 457.
- [18] Zhukov A.V., Bouffanais R., et al. Collisions of three-dimensional bipolar optical solitons in an array of carbon nanotubes. *Phys. Rev. A*, 2016, **94**, 053823.
- [19] Ferray M., L'Huillier A., et al. Multiple-harmonic conversion of 1064 nm radiation in rare gases. *J. Phys. B: At. Mol. Opt. Phys.*, 1988, **21**, L31.
- [20] Chang Z., Rundquist A., et al. Generation of Coherent Soft X Rays at 2.7 nm Using High Harmonics. *Phys. Rev. Lett.*, 1997, **79**, 2967.